

Austral Summer MJO Forecast Skill in S2S Models: Decadal Shifts and Their Drivers

Raina Roy ^{a,b,*}, Julie M. Arblaster ^{a,b}, Matthew C. Wheeler ^c, Eun-Pa Lim ^c, Jadwiga H. Richter ^d

^aSecuring Antarctica's Environmental Future, Monash University, Clayton, VIC, Australia

^bSchool of Earth, Atmosphere and Environment, Monash University, Clayton, VIC, Australia.

^cResearch, Bureau of Meteorology, Melbourne, VIC, Australia.

^dNational Center for Atmospheric Research, Boulder, Colorado, USA

VAR model

We employ a Vector Autoregressive (VAR) model, following Marshall et al. (2016) and Maharaj & Wheeler (2005), to establish a baseline for MJO predictability independent of dynamical model complexities. The model predicts future RMM1 and RMM2 indices using their lagged values through the coupled equations:

VAR System:

$$RMM1(t) = \alpha_1 + \beta_{11}RMM1(t-1) + \beta_{12}RMM2(t-1) + \varepsilon_1(t)$$

$$RMM2(t) = \alpha_2 + \beta_{21}RMM1(t-1) + \beta_{22}RMM2(t-1) + \varepsilon_2(t)$$

Where:

- α_1, α_2 are intercept terms,
- β_{ij} are the coefficients quantifying the influence of lagged RMM1 and RMM2,
- $\varepsilon_1(t), \varepsilon_2(t)$ are residuals (white noise).

The coefficients (α, β) are estimated using multivariate (multiple) linear regression on historical observations. They are computed separately for each period (e.g., 1981–1998 and 1999–2018) to allow for possible changes in the system's dynamics over time. The equations of the model used for our study are shown below:

For the first period (1981-1998):

$$RMM1_t = 0.9450 (RMM1_{t-1}) - 0.1131 (RMM2_{t-1})$$

$$RMM2_t = 0.1211 (RMM1_{t-1}) + 0.9820 (RMM2_{t-1})$$

For the second period (1999-2018):

$$RMM1_t = 0.9405 (RMM1_{t-1}) - 0.1088 (RMM2_{t-1})$$

$$RMM2_t = 0.1352 (RMM1_{t-1}) + 0.9824 (RMM2_{t-1})$$

36

37 Bivariate Anomaly Correlation

38

39 The bivariate anomaly correlation is estimated using the following formula:

$$COR(\tau) = \frac{\sum_{t=1}^N [RMM1(t) rmm1(t, \tau) + RMM2(t) rmm2(t, \tau)]}{\sqrt{\sum_{t=1}^N [rmm1(t, \tau)^2 + rmm2(t, \tau)^2]} \sqrt{\sum_{t=1}^N [RMM1(t)^2 + RMM2(t)^2]}}$$

41

42 Here, RMM1 and RMM2 are observed MJO indices, and rmm1 and rmm2 are forecasted MJO
43 indices.

44 MJO amplitude is computed using the following formula:

$$MJO \text{ Amplitude } obs(t) = \sqrt{\sum_{t=1}^N [RMM1(t)^2 + RMM2(t)^2]}$$

$$MJO \text{ Amplitude } model(t, \tau) = \sqrt{\sum_{t=1}^N [rmm1(t, \tau)^2 + rmm2(t, \tau)^2]}$$

47 MJO Skill Index Calculation Method

- 48 1. Bivariate Correlation Computation
- 49 For each initialisation date (12 start times per DJF season), calculate the 40-day lead
- 50 bivariate anomaly correlation (B. Corr) between:
 - 51 a. Observed RMM1/RMM2 indices (OBS)
 - 52 b. Forecasted rmm1/rmm2 indices (FCST)
- 53 2. 15–25 Day Skill Averaging
 - 54 a. For each year, compute the mean skill index by averaging correlations across
 - 55 lead times of 15–25 days.
- 56 3. Temporal Aggregation
 - 57 Repeat Steps 1–2 for all austral summer seasons (DJF) across:
 - 58 a. Period 1: 1981–1998 (18 years)
 - 59 b. Period 2: 1999–2018 (20 years)
- 60 4. Multi-Model Analysis
 - 61 Apply this method uniformly to:
 - 62 a. Dynamical Models: ACCESS-S2, POAMA2, CESM2, GEOS-S2S-2
 - 63 b. Statistical Benchmark: VAR model ensuring cross-comparable skill metrics.

MJO Event estimation

MJO events are calculated using a method that differs slightly from that of Wei & Ren (2019). The steps are as follows:

1. Day 0 of the event can begin in any phase of the MJO.
2. The MJO amplitude must remain above 1 for the next seven consecutive days. This criterion helps identify events that have a strong start.
3. Once the first criterion is met, the MJO must progress in an anticlockwise direction to at least two of the following phases. For our analysis, we have considered both propagating and non-propagating MJO events.

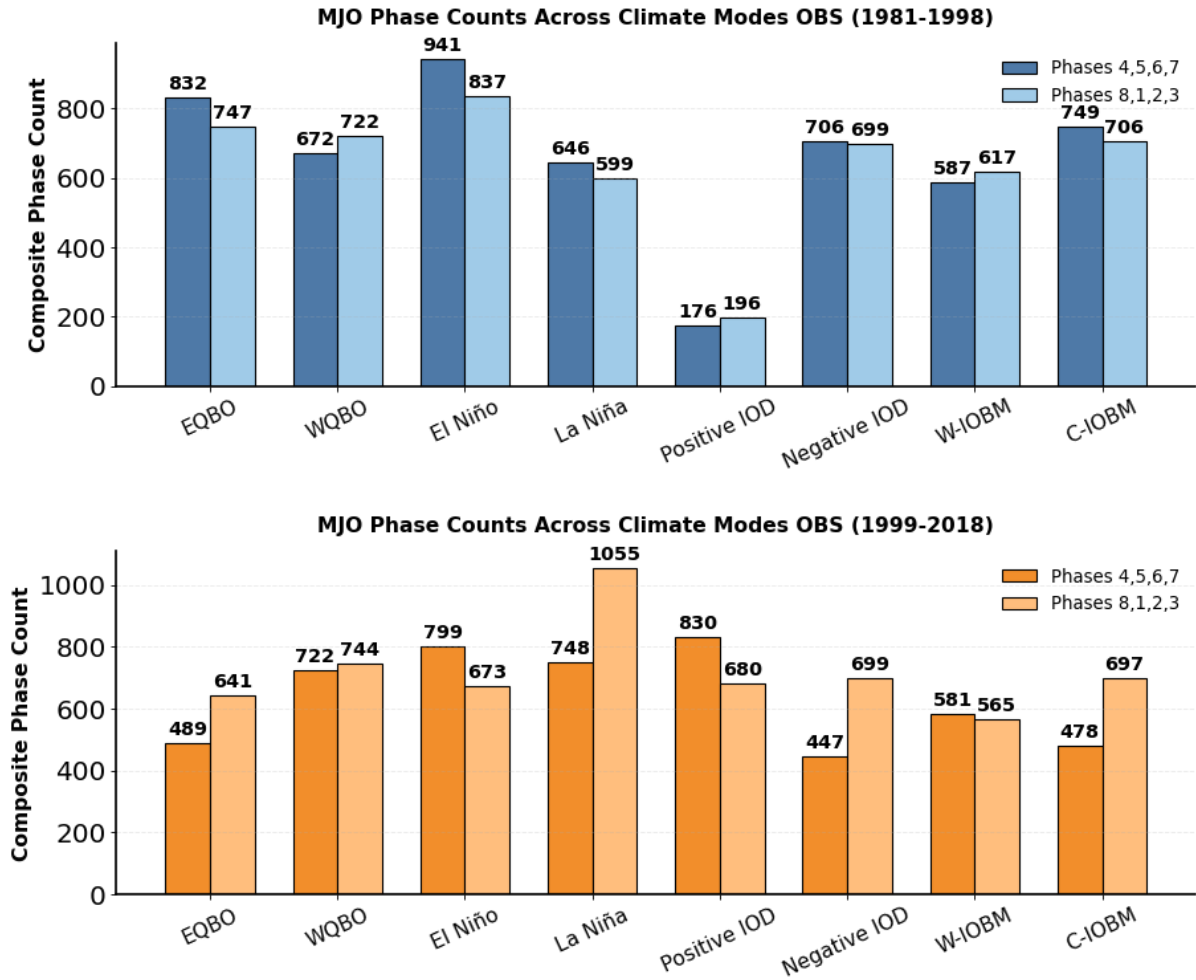


Figure S1. Composite MJO phase frequency distribution for 1981–1998 (row 1) and 1999–2018 (row 2), showing distinct modulation by climate mode phases. Phases 3–6 demonstrate the occurrence in the Eastern Indian Ocean to the Maritime Continent region. Phases 7-2

79 show the occurrence in the eastern Pacific to the Western Indian Ocean region.
80